Multi-Harmonic Identification with Swept-Sine Excitation in Nonlinear Dynamics

Eduardo Sousa
eduardo.sousa@tecnico.ulisboa.pt

Instituto Superior Técnico, Universidade de Lisboa, Portugal

November 2022

Abstract

The Digital Tracking Filter (DTF) is a technique to obtain good estimations of the amplitude and phase of the measured response of the system and applied force, and hence of the structural Frequency Response Functions (FRFs), under swept-sine excitation. It is normally more accurate than the harmonic estimator in presence of tonal disturbances. The goal of this work is to extend the DTF procedure to nonlinear structures. Indeed, while the response of a linear structure manifests only at the fundamental excitation frequency ω, a nonlinear structure vibrates also at integer multiples of ω, $n \times \omega$, called harmonics. The proposed technique, labelled Multi-Harmonic Digital Tracking Filter (MHDTF), estimates the amplitude and phase of these higher-orders harmonics as well. The procedure is first applied to simulated data and compared with the harmonic balance (HB) method estimations. Then, experimental data are also analyzed, and the results are compared with the ones of an adaptive filter.

The multi-harmonic capabilities of the MHDTF open the way to its potential use in the nonlinear system identification area. In this context, the methodology of obtaining a multi-harmonic State-Space model is described and used for time simulations. The procedure is applied to a demo airplane experimental setup. The advantage of this approach is its simple use and the possibility to better approximate a response with multi-harmonic contributions. The clear drawback lies in the linearisation, hence, its accuracy only at the level of excitation used during the identification. **Keywords:** Nonlinear System Identification, Higher-order harmonics, Nonlinear Frequency Response Curve, Dynamic Testing, Digital Filter, Multi-harmonic State-space Model.

1. Introduction and Theoretical Background

Understanding the dynamical behaviour of a mechanical system is key in the pursuit of reliable, cheaper and more efficient structures that positively affect the world.

A frequency response function (FRF) in structural dynamics is a complex frequency domain function that describes response of a point per unit force at the input location [1]. The FRF can be obtained analytically, assuming previous knowledge of the mathematical model of the system, or experimentally. In experimental testing, the input and output data of a structure subjected to dynamic forcing is measured.

The current work is pivoted on the analysis of swept-sine excited structures. This type of excitation is able to excite most of the resonances of the system, as long as they are in the excitation bandwidth, while ensuring a good trade-off between magnitude of excitation level and testing time [2].

Processing the response of the structure in order to estimate the amplitude and phase of this signal is vital in undertaking system identification. Furthermore, paired with the $H1$ estimator, the FRF of the structure is then constructed. An accurate estimation of the force and the response amplitude and phase during a structural acquisition is a key process to obtain good quality FRFs [1].

The harmonic estimator is a tracking technique already rooted in the industry, simple and effective. The Digital Tracking Filter (DTF) fulfills the same purpose as the harmonic estimator yet it has shown to reject more efficiently disturbances in the signal [3]. Both techniques take advantage of the known time-frequency relation of swept-sine testing.

The DTF, with previous developments carried in [3], has the capability of tracking the fundamental harmonic, that contains the same procedure as the widely electronics industry used lock-in amplifier [4]. The procedure, pictured in Figure 1, is carried out in three stages: dual-phase homodyning, followed by lowpass filtering and amplitude and phase extraction.

Dual-phase homodyning is the first stage. The response signal is mixed with two Constant Output Level Amplitude (COLA) reference signal with the

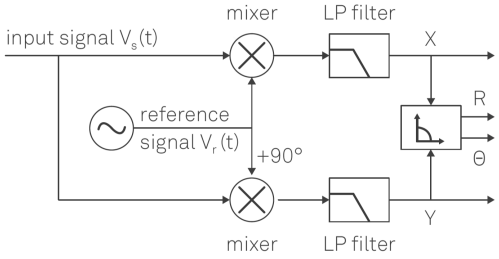

Figure 1: MHDTF procedure diagram.

same frequency content of the response/excitation, one of them shifted by 90°:

$$resp\_signal(t) \times \sin(\omega \times t) = \frac{1}{2}A(t)\big(\cos(\phi(t)) - \cancel{\cos(2\omega \times t + \phi(t))}\big) \quad (1)$$

$$resp\_signal(t) \times \sin(\omega \times t + 90°) = \frac{1}{2}A(t)\big(\sin(\phi(t)) + \cancel{\sin(2\omega \times t + \phi(t))}\big) \quad (2)$$

The outcome of each mixing, or homodyning, can be separated into two new homodynes, that is, two new signal frequencies: a DC component, at 0 Hz, and a $2\times\omega$ component, with all the required tracking information easily obtained from the DC components.

The lowpass filtering is the following stage, aiming to attenuate all components above DC: the $2\times\omega$ homodyne component and all other disturbances in the signal.

Following the filtering stage, only the DC homodynes remain. The DC component originated from Equation 1 and Equation 2 are labelled in-phase and quadrature respectively, from which the amplitude and phase are obtained.

The DTF is best suited for linear systems. Nonlinear systems, instead, exhibit a much more complex response with diverse nonlinear phenomena [5] [6]. One of the most relevant phenomena is the multi-harmonic response for single-harmonic input, particularly at integer multiples of the fundamental excitation frequency, called harmonics.

Although methods to identify this multi-harmonic content are already present in the literature, as for instance the adaptive filter [7], the motivation of this work is to take advantage of the DTF suitability in processing data in presence of noise and tonal disturbances, and extend its use to a multi-harmonic identification. The goal is then to build a solid identification method, the Multi-Harmonic Digital Tracking Filter (MHDTF), to identify the different harmonics response, in a robust and reliable way, during MIMO swept-sine testing of complex structures.

In this paper, first, the estimations of the MHDTF are compared with the ones of the HB method, a numerical method that approximates the steady-state response of a system with known properties as the summation of a definite number of harmonics. The specific HB method implementation used in this work can be found in [8]. Secondly, experimental data of an airplane with nonlinear properties are analyzed, and the estimations of the MHDTF are compared with ones of an adaptive filter [7], a data-driven method based on a least mean squares (LMS) algorithm.

2. Implementation

The MHDTF procedure is summarized in Figure 2. In this section, each block of the diagram is briefly introduced and explained.

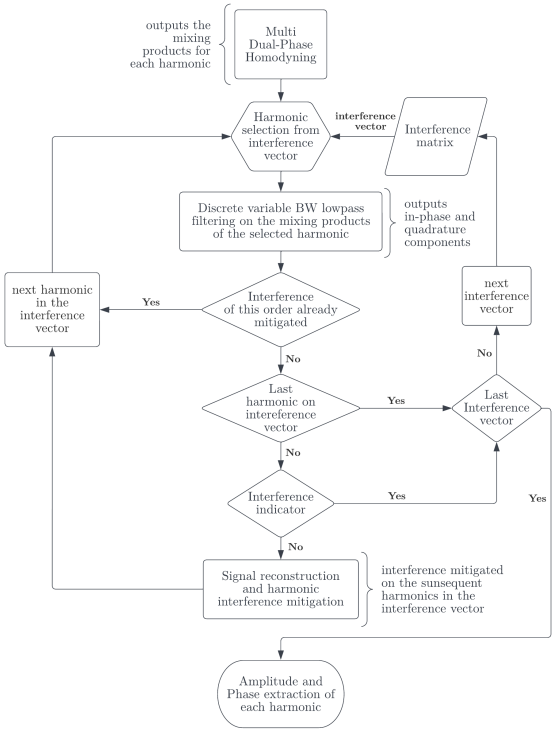

Figure 2: MHDTF procedure diagram.

2.1. Multi Dual-Phase Homodyning

The MHDTF procedure starts with the multi dual-phase homodyning. Since the response of a nonlinear structure is composed not only of the fundamental frequency but also of its harmonics, the homodyning mixing products differ from the single harmonic homodyning of Figure 1.

For illustration, a multi harmonic example signal, with two components, is defined: fundamental component at 10 Hz, with unit amplitude and null phase and a 2^{nd} harmonic component, trivially at 20 Hz, with half unit amplitude and null phase. The Fourier transform of this signal is in Figure 3.

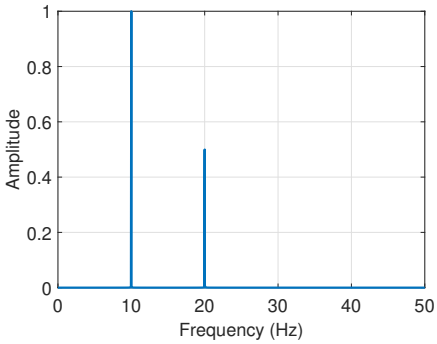

Figure 3: Fourier transform of example signal before mixing.

The mixing products of this signal with the reference signal, $ref\_signal(t) = \sin(\omega \times t)$, provide two homodynes, at DC and 20 Hz, and also two heterodynes, at 10 Hz and 30 Hz, as visualized in Figure 4.

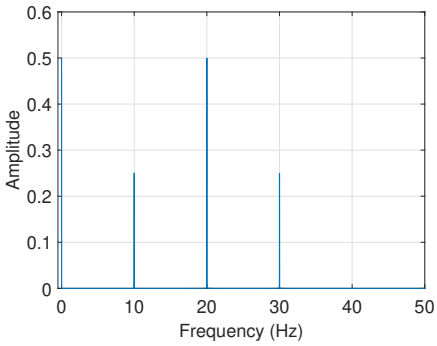

Figure 4: Fourier transform of example signal after mixing at ω.

In general, the mixing product of the multi harmonic response signal with the reference signal, as well as the 90° phase shifted reference signal, will contain two homodynes and as many pair of heterodynes as there are higher order harmonics in the response signal. The products of this dual-phase homodyning with the COLA reference signals at the fundamental frequency contain information regarding the 2^{nd} harmonic, at the heterodynes. However, it is more convenient to also perform a dual-phase homodyning targeted at the 2^{nd} harmonic order, in an effort to bring the respective harmonic content to DC where it is more easily extracted after the lowpass filtering.

Therefore, mixing the original signal in Figure 3 with a COLA reference signal at double the fundamental frequency, $ref\_signal(t) = \sin(2\omega \times t)$ provides the Fourier transforms in Figure 5.

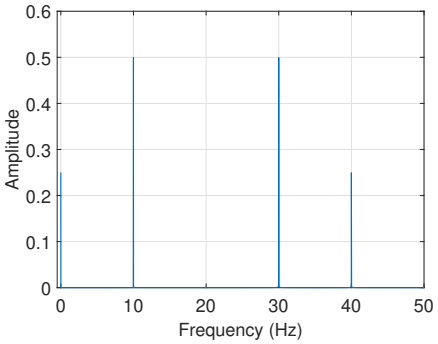

Figure 5: Fourier transform of example signal after mixing at 2ω..

As observed, there are two homodynes, at DC and 40 Hz, and two heterodynes, at 10 Hz and 30 Hz, the latter resultant of the mixing with the fundamental harmonic component of the response signal. Ultimately, the multi dual-phase homodyning stage of the MHDTF procedure provides for a pair of mixing products per harmonic order, with the content of the respective harmonic conveniently situated at 0 Hz but also at $h\_order \times 2f$, with other pairs of heterodynes respective to the other harmonic orders also present. Of course, more heterodynes may appear due to noise in the signal, and tonal disturbances. This multitude of homodynes and heterodynes is very relevant as they may interfere with each other and perturb the amplitude and phase estimation.

2.2. Discrete Variable Bandwidth Lowpass Filtering

In this stage, ideally, all frequencies above DC are filtered out. The parameters of the employed lowpass filter influence the tracking accuracy and an optimal design is required to ensure the best outcome. The most influential parameters are: design method, filter order and cut-off frequency.

The design method implemented in the development of the MHDTF is the Butterworth design. As suggested by [9], the Butterworth design is versatile and offers a smooth monotonic frequency response that is maximally flat in the passband.

The filter order also plays a significant role in the performance of the filter. Increasing the filter order improves unwanted components rejection, as the transition of the filter is steeper at a cost of a slower filter response.

Another trade-off choice must be made on the cut-off frequency. Lower cut-off frequencies reject unwanted homodyne, heterodyne and noise components more efficiently, but perform slower. Since the filtering purpose is to attenuate all frequencies above DC, delineating the cut-off frequency evolves around this purpose. Previous studies [3]

on the single-harmonic DTF have shown that the cut-off frequency, f_c, is optimal in the vicinity of 15% of the lowest signal frequency, f_0, for good response and noise rejection, $f_c/f_0 \approx 0.15$. For multi-harmonic purposes, this cut-off ratio is updated to the lowest signal frequency of the respective harmonic, $f_c/(h\_order * f_0) \approx 0.15$.

More importantly, for swept sine excitation, as the signal frequency increases, the constant pass-band bandwidth imposed by this cut-off ratio results in poor filter performance at higher frequencies. Therefore, a variable bandwidth filter should be employed to assure tracking quality, with the cut-off frequency evolving at the same pace of the sweeping frequency, f, to which the notion of cut-off ratio is redefined as the ratio of the cut-off frequency and the sweeping frequency of the specific harmonic order to track, $f_c/(h\_order * f) \approx 0.15$.

Regarding the filter itself, although there are already solutions to create varying bandwidth filters [10], the employed method is much more discrete and simple, aiming to use the MATLAB *filtfilt* function, that performs zero-phase digital filtering by processing the input data in both the forward and reverse directions. It allows the use of higher filter orders and lower cut-off ratios without performance loss.

The method consists in dividing the entire sample interval in N sub-intervals (Figure 6). For optimal results and computation efficiency, the number of sub-intervals, N, must be correlated to the excitation bandwidth, since the decrease in performance at the end of the sub-interval occurs for increased frequency differences between the start and end of the sub-interval.

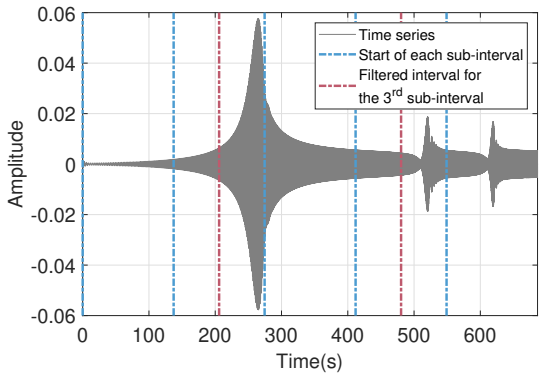

Figure 6: Response divided in 5 sub-intervals, $N = 5$, equally divided in samples/time. The red lines represent the wider interval for the 3^{rd} sub-interval.

Additionally, another relevant discrete varying filtering detail emanates from the delay and poor performance associated with the start and end of each filtering cycle. Therefore, a wider interval must be filtered and then the correct sample allocation must be done to the original sub-interval. The best trade-off for the current application is a 4^{th}-order filter with a cut-off ratio of 15% of the sweeping frequency. The latter can possibly be scaled downwards to 10% without any major estimation drawbacks.

Harmonic Interference Mitigation

Harmonic interference mitigation is an extra stage of this procedure that rises solely from the multi harmonic content of the nonlinear responses. The clearest way to demonstrate the need of this mitigation is to apply the described multi-harmonic identification procedure on a single harmonic signal. Theoretically, without interference, the higher-order harmonics content is expected to be irrelevant.

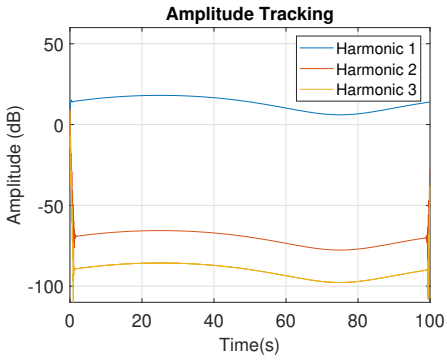

Figure 7: Multi-harmonic amplitude tracking of single-harmonic swept-sine, without interference mitigation, N = 1, cut-off ratio = 15%.

Instead, Figure 7 shows that the tracking of the 2^{nd} and 3^{rd} order harmonics is not null. This is due to the influence of the 1^{st} harmonic heterodyne on the mixing products of the 2^{nd} and 3^{rd} harmonics, as the curves similar shape of the curves might suggest. The influence on the 2^{nd} harmonic is greater than the 3^{rd} because the 1^{st} harmonic heterodyne is further away from DC for the 3^{rd} harmonic homodyning products than for the 2^{nd} harmonic products.

Decreasing the amplitude of the fundamental harmonic, which is the interfering harmonic in this situation, also decreases the interference curves by the same amount, which is an indicator of the primary influence of the difference between the higher and lower amplitude harmonics. Concluding, harmonic interference arises from all the heterodyne products resultant of the multi dual-homodyning stage. All orders interfere with each other. It is only when the amplitude difference between these orders is very large that there is a need to mitigate this phenomena.

The current method for the harmonic interference mitigation is to recreate the interfering single harmonic order signal and then subtract the heterodyne products of this recreated single harmonic signal with the different order reference signals to the mixing products of the initial dual-phase homodyning stage. Ultimately, this is identical as eliminating the interfering component from the response signal and then perform the dual-phase homodyning of the interfered orders, but much more compact.

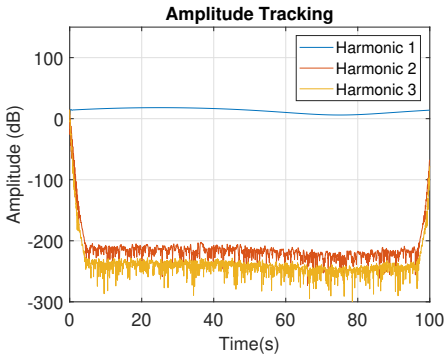

Figure 8: Multi-harmonic amplitude tracking of single-harmonic swept-sine, with interference mitigation, N = 1, cut-off ratio = 15%.

The mitigation is not fully achieved in Figure 8, since the recreated single harmonic signal is only an approximation of the single harmonic signal itself. However, it does allow to lower the interference level so that the resultant amplitude estimation of the higher orders that reside below this cap are clear to the user as erroneous, in contrast to the previous amplitude estimation that could induce in error.

For swept-sine excitation, when $N > 1$ (Figure 6), it is possible to use an interference indicator to verify if the amplitude tracking of a certain harmonic order is composed or not of interference. This indicator operates by verifying the initial sample of a filtering interval and the previous sample, and assessing the difference in amplitude between these two points. If this difference is bigger than a defined amount, as in Figure 9, at 20 Hz, 30 Hz and 40 Hz for the 2^{nd} and 3^{rd} harmonic orders, the interference is detected.

These amplitude leaps occurs due to the different cut-off frequencies of each sub-interval. As the cut-off frequency increases for the next sub-interval, it instantly rejects less the interfering heterodyne, which causes the sudden increase in amplitude. This method has proven sufficient enough in the assessment of harmonic interference and remains tunable by the user according to the obtained results.

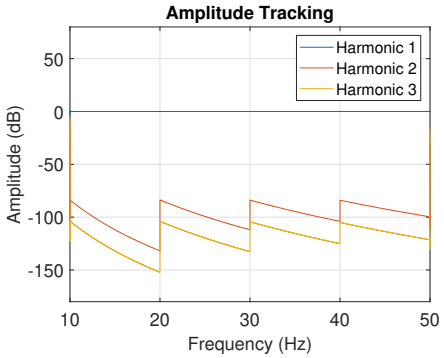

Figure 9: Multi-harmonic amplitude tracking of single-harmonic swept-sine, without interference mitigation, N = 4, cut-off ratio = 15%.

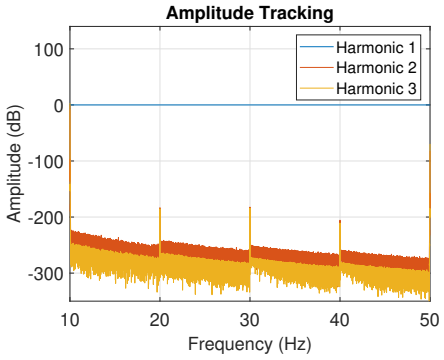

Figure 10: Multi-harmonic amplitude tracking of single-harmonic swept-sine, without interference mitigation, N = 4, cut-off ratio = 15%.

To tie the interference indicator in a procedure that evaluates and mitigates interference, the information on which harmonic interferes with the others is required. This information is stored in the interference vector. For illustration, a vector as [1 2 3] delineates that the 1^{st} harmonic interferes with the 2^{nd} and the 3^{rd}. Additionally, the 2^{nd} harmonic interferes with the 3^{rd}. The mitigation procedure follows this same order. The interference of harmonic 1 is mitigated on harmonic 2 and 3 and the interference of harmonic 2 is mitigated on harmonic 3. An interference matrix is then composed of several interference vectors, resultant of the permutation of the several harmonic orders, with the fundamental order always being the 1^{st} order of each vector.

From this, the mitigation procedure on Figure 2 focuses on rejecting the interference vectors that have the wrong interference order and trying to find the most appropriate vector. It is also important to reassure in this procedure that the interference that one harmonic causes on the others is only mitigated once.

3. Results on simulated data

The 3-degrees-of-fredom (DOFs) system in Figure 11, whose properties are depicted in Table 1 and Table 2 is analyzed.

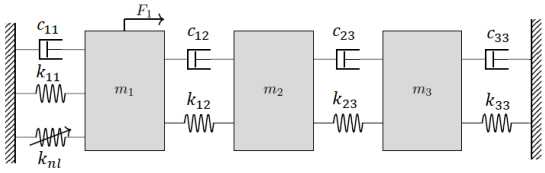

Figure 11: 3-DOF system. Cubic spring at the 1^{st} mass is the source of nonlinearity.

Table 1: 3-DOF system parameters (I).

Mass(Kg)	Stiffness (N/m)
$m_1 = 10$	$k_{11} = 1$
$m_2 = 1$	$k_{12} = 3$
$m_3 = 1$	$k_{23} = 1$
	$k_{33} = 1$

Table 2: 3-DOF system parameters (II).

Nonlinear cubic stiffness (N/m^3)	Damping (Ns/m)
$k_{nl} = 1$	$c_{11} = 0.3$
	$c_{12} = 0.01$
	$c_{23} = 0.01$
	$c_{33} = 0.01$

From one side, these properties are processed with the HB method, providing a steady-state solution that establishes a great benchmark to compare to the MHDTF results. On the other side, the system is excited with a swept-sine and the response is retrieved using the Newmark solver. The input-output data are then processed with the MHDTF, following the already described procedure. The same excitation amplitude (0.05 N) and location (mass 1) is used in both cases.

The results of the comparison are shown in Figure 12. The amplitude of the displacement, expressed in dB, and the absolute phase, in degrees, of DOF 1 of the described system is portrayed, for the 1^{st} and 3^{rd} harmonic orders. By virtue of the cubic nonlinearity, these two harmonic orders are the most significant.

In the results comparison there is a clear correspondence between the two responses for both harmonics down to the -250 dB amplitude level, where the tracking of harmonic 3 is clearly corroded. This can be due to the tolerance error used in the Newmark simulation, transient and in general the difference between 1^{st} and 3^{rd} harmonic-order amplitude. Furthermore, there is no interest in estimating such a low response contribution, also because in experimental measurements the signal-to-noise ratio is expected to be lower than 190 dB.

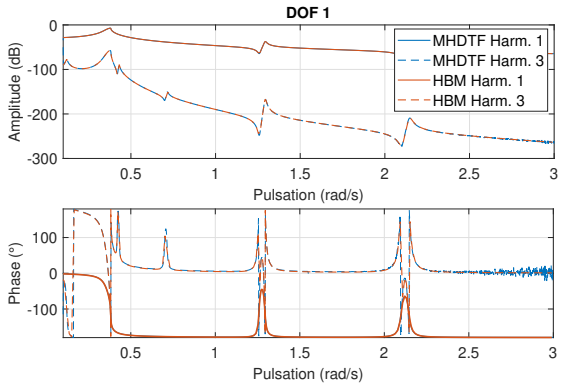

Figure 12: DOF1 displacement amplitude and phase of 1^{st} and 3^{rd} harmonic order per HB method and MHDTF tracking.

4. Experimental Results

The experimental setup of an airplane mock-up is shown in Figure 13. Despite of the simple design, its dynamic behavior presents several complex nonlinear phenomena. The source of nonlinearity are mainly the two pylons under the wings, but also the bolted connections between the different components. The measurements of both input and output data is recorded using force cells and accelerometers. These are situated on the wing, fuselage, horizontal and vertical tail, and on the pylon masses. The airplane is excited at approximately midway of each wing, with electrodynamical shakers, under swept-sine excitation. The bandwidth of excitation is 5 to 110 Hz.

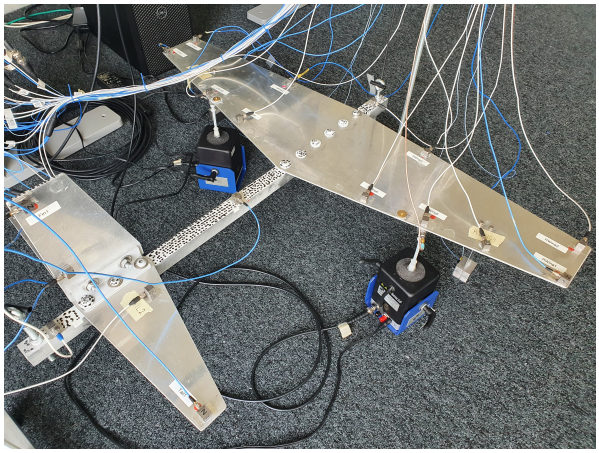

Figure 13: Experimental setup.

From the measurements of both the input force and acceleration signals, two tracking methods, the adaptive filter and the MHDTF, are applied, allowing the calculation of the nonlinear frequency re-

sponse curve (NLFRC) utilizing the $H1$ estimator.

It is important to remark that the noise disturbance can be more significant than the harmonic interference. Therefore, for computation efficiency, the harmonic interference mitigation stage is ignored in the shown identifications.

The structural NLFRC is plotted in Figure 14 for the two methods, in dB. LPyl1 is the point on the top mass of left pylon while LWing4 is the driving point in the middle of the left wing. The estimations of harmonic 1 are clear and identical for both methods, except in the vicinity of 45 Hz. Harmonic 2 and 3, due to their lower amplitude, are more subjective to disturbances in the signal.

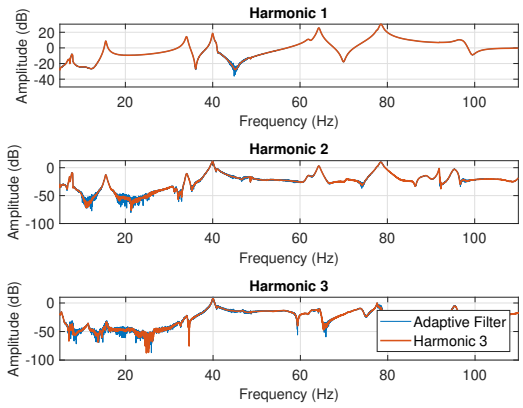

Figure 14: NLFRC amplitude estimation for left_pylon_1/left_wing_4.

The MHDTF is more effective in rejecting these disturbances when comparing to the adaptive filter. This is evident for harmonic 1, at around 45 Hz, and for harmonics 2 and 3 all across the bandwidth. The MHDTF cut-off ratio utilized is 10%, which has proven to be the inferior limit for tracking accuracy and optimal noise rejection. However, in the frequency range between 5 and 30 Hz, and especially at around 26 Hz for harmonic 3, the MHDTF is not fully capable of attenuating the noise.

In Figure 15, the measured acceleration signal is plotted together with the amplitude of the tracked harmonics 1, 2 and 3 from the MHDTF, and their sum. RPyl2 is one of the two points at the bottom mass of right pylon. It is very noticeable how the higher-order harmonics contribution becomes significant when resonances are excited. In particular, at 7.6 Hz and 48.5 Hz, the harmonic sum much better approximates the time series amplitude, and, at 40.6 Hz and 44.3 Hz, harmonic 2 is even larger than harmonic 1. The identification error that is committed in identifying the fundamental harmonic only is hence very clear.

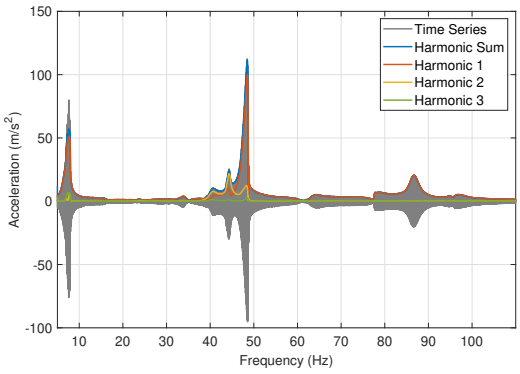

Figure 15: RPyl2 acceleration signal and MHDTF estimations.

5. Multi-Harmonic State-Space Modelling

Hugely facilitated by state-of-the-art tools in the linear system identification and modal analysis fields, many conveniently embedded in the Siemens Testlab software, the proposed methodology attempts to linearise a nonlinear structure, through its harmonic estimations provided by the MHDTF, and create a multi-harmonic State-Space (SS) model. The advantage of this approach is its simple use and the possibility to better approximate a response with multi-harmonic contributions. The clear drawback lies in the linearisation, hence, its accuracy only at the level of excitation used during the identification.

5.1. Theoretical Synopsis

The employed techniques are briefly introduced: PolyMAX and Maximum Likelihood estimation of a Modal Model (MLMM) algorithm to obtain the modal model and then the posterior conversion to SS model.

5.1.1 PolyMAX and MLMM

PolyMAX is referenced as a new standard for modal parameter estimation, as introduced in [11]. It is a non-iterative frequency-domain parameter estimation method based on a weighted least-squares approach. It constructs a modal model, by extracting, from MIMO FRFs, a meaningful set of modes and their associated modal parameters including: natural frequencies, damping values and mode shapes.

PolyMAX relies on modal fitting process, comparable to that used for curve fitting. Different polynomial orders are tested during the curve fitting process, and the polynomial coefficients are then calculated to reduce the discrepancy between the curve and the data. Similar steps are taken in the calculation of modal curves, where varying numbers of modes are taken into account before determining the modal shapes, natural frequencies, and modal damping values to best match the measured FRFs.

Shortly, PolyMAX, in its procedure, starts with the creation of a stabilization diagram containing frequency, damping and participation information. From here, the modal modes are selected, either by the user or automatically. A faithful mode selection is important, they must correlate the modes from the inputted FRFs. Validation of the obtained modal model can be obtained with the comparison of the synthesized FRFs, as constructed from the modal model, and the originally inputted FRFs.

In order to improve the fit of the modal model, that is, a better match of the synthesized FRFs, the MLMM algorithm can be employed [12]. MLMM automatically iterates on the parameters of the initial modal model to optimize the fit between the identified model and the inputted FRFs.

5.1.2 State-Space and Modal Model Conversion to Modal State-Space Model

The SS model is a method of representing dynamical systems. It transfers observations of a response variable to unobserved states or parameters by an observation model. These state variables describe a system of first-orders differential equations, reducing its complexity.

The continuous-time state space model consists of Equation 3a, state equation and the observation equation, Equation 3b. The calculated output response, in the time domain, $y \in \mathbb{R}^{n_o \times 1}$ is calculated as a function of the n internal states vector $x \in \mathbb{R}^{n \times 1}$ of the system through the output matrix $C \in \mathbb{R}^{n_o \times n}$ and of the input vector $u \in \mathbb{R}^{n_i \times 1}$ through the direct throughput matrix $D \in \mathbb{R}^{n_o \times n_i}$. In this case, D is null. $A \in \mathbb{R}^{n \times n}$ corresponds to the state matrix and $B \in \mathbb{R}^{n \times n_i}$ to the input matrix.

$$\dot{x} = Ax + Bu \tag{3a}$$

$$y = Cx + Du \tag{3b}$$

The pairing of the modal and State-Space model is covered in depth in [13].

5.2. Methodology and Guidelines

It is easier to first introduce the procedure and outcomes for linear systems and then dive into the nonlinear implications and consequent changes.

Briefly, the response time series contain the behaviour of the structure to a specific input force. This behaviour is then generalized in the FRFs. From here, the curve fitting algorithm creates the modal model that best approximates these FRFs and therefore the structure itself. This model is converted to a SS model, in the aforementioned A, B and C matrices. From Equation 3, only the input force u is missing to calculate the simulated time response y. In structural utopia, if the same input vector that originated the time series and FRFs of the system is provided to the SS simulation, y matches the response time series. Additionally, different input force u should numerically predict the actual response of the structure to the same u.

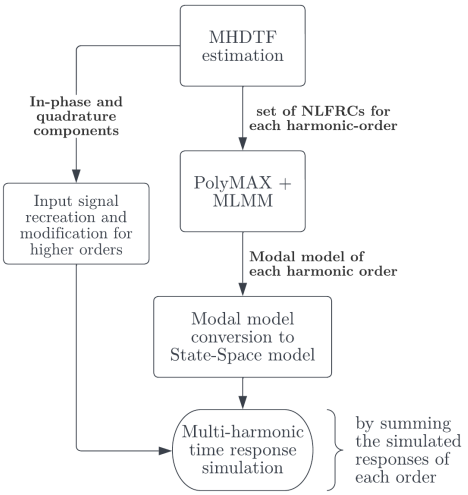

Figure 16: Multi-harmonic State-Space modelling and simulation procedure.

The first predicament of nonlinear systems is that they respond at also its harmonics. Second predicament is that the concept of FRF falls. The behaviour of the structure is not generalized and the NLFRCs are only specific to the input force that generated it. Therefore, predicting the behaviour of the response of the system to different inputs than the one that originated this modal system will not lead to good predictions.

The proposed procedure of multi-harmonic SS modelling and respective time domain simulation is proposed in Figure 16.

5.2.1 MHDTF Estimation

Utilizing the MHDTF is the first step. The time series, either simulated or acquired from experimental testing, are processed. The purpose is to obtain a set of high-quality NLFRCs for each tracked harmonic.

Additionally, if the simulated time response objective is to compare its results to the time series that originated it, the MHDTF also has the purpose of providing the in-phase and quadrature components of harmonic 1.

5.2.2 PolyMAX + MLMM

Following, the modal models of each harmonic order are obtained utilizing PolyMAX. In a nutshell, each harmonic order is processed as its own individual

system to process, with its own modal model and respective modal parameters.

In this framework, modal validation from the perspective of the user should focus on obtaining a proper fit of the synthesised FRFs, as the modeset and consequently MAC validation have a secondary value in this application. The fit really is of primary importance to have good time predictions. While this has proven to be fairly achievable for the fundamental harmonic, the higher orders have proven to be quite troublesome, since the NLFRCs can be corroded by noise or harmonic interference. Additionally, using a curve fitting method designed for linear systems on nonlinear systems can contribute to the poor modal validation. In this context, the user should guide the fit towards the modes with higher amplitude as these are the main contributors in the grand scheme. In a way, with the employment of MLMM, this is already done, since this algorithm may shift several modes to one resonance.

5.2.3 Multi-Harmonic State-Space Response Simulation

The input force time series given to the simulations is the non-orthodox aspect of this methodology. First, it is important to remark that nonlinear system responds at the frequency ω and also at its harmonics for a single-harmonic input at ω. Therefore, this multi-harmonic SS model should react in the same fashion, introducing a single-harmonic input at ω should provide a multi-harmonic time response. As previously stated, each harmonic order is its own SS model from which the time simulated responses of each order are calculated, summing up all these responses to this single-harmonic input must provide the desired outcome. However, the SS simulation is linear, introducing an input signal at frequency ω will always output a response at ω. It is easy to see how this becomes problematic for the higher orders, since the input force at ω will not lead to a response at $h\_order \times \omega$.

Therefore it is required that the input of the higher-orders simulations is manifested in its correct BW. The frequency of the input must be modified. In the case of simple constant spectrum inputs with a known frequency content, this modification is trivial. Otherwise, for the simulation of a specific harmonic-order, the instantaneous Fourier coefficients of harmonic 1, or in-phase and quadrature components, previously retrieved from the initial MHDTF processing, are multiplied with Constant Output Level Amplitude (COLA) reference signals of the respective order, as in Equation 4, resulting in a signal with the same amplitude and phase content of the original harmonic 1 recreated signal, but at the desired multiple of its frequency.

$$input\_force_h(t) = in-phase_1(t) \times \sin(h \times \omega \times t) + quadrature_1(t) \times \sin(h \times \omega \times t + 90°) \quad (4)$$

The obtained signal is used as input for the simulation of the h^{th} order SS model. After, the responses from each SS model, i.e. from each order, are summed respecting the initial relation between excitation frequency and response frequencies, leading to the desired multi-harmonic simulated response.

5.3. Application on a Demo Airplane Experimental Setup

The experimental setup to be modelled is the same as discussed in section 4, where it was shown to present a strong harmonic 2 and 3 contribution.

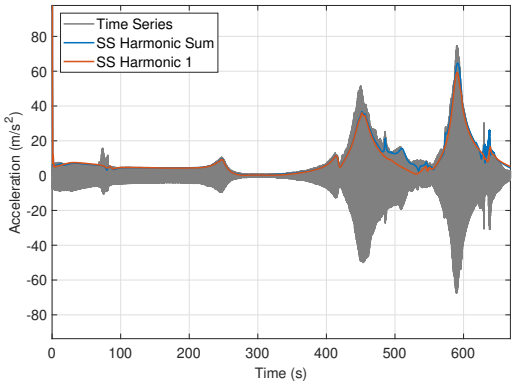

Figure 17: LWing6, sweep 1 measured response contrasted with state-space simulation harmonic sum and harmonic 1 amplitudes.

The procedure starts with the measured signals MHDTF processing. After, PolyMAX and MLMM were utilized. The fits of harmonic 1 were overall very adequate. Harmonics 2 and 3 were inferior but still optimal since the experimental model has the advantage of having a strong higher-order contribution that facilitates PolyMAX's work. However, the model fit has shown to be not good when disturbances are present in the NLFRCs.

The harmonic sum and harmonic 1 amplitudes of the SS simulated time response are contrasted with the measured time series in Figure 17. It is possible to see, not only the accuracy of the SS model, by comparing the time series with the harmonic sum, but also the improvement of including higher-order harmonics in the model by comparing the harmonic sum and the harmonic 1 amplitudes. In general, better predictions were obtained where the fits were best.

6. Conclusions

The MHDTF is proven to be a very efficient tool to estimate the multi-harmonic response of a nonlin-

ear system under swept-sine excitation. The contribution of the higher-order harmonics can be significant, especially in case of modal interactions. First, it is validated on a simulation system using the harmonic balance method for comparison. Then, its estimations are compared with the ones of an adaptive filter, processing experimental data corrupted by nonlinearity and noise. The very good suitability of the DTF to reject noise disturbances is kept in its multi-harmonic extension. Future developments on the MHDTF should focus on the lowpass filtering stage. In the end, this is where the good disturbance attenuation capabilities of this technique originate from. Additionally, the MHDTF identification of sub-harmonics is yet to be explored.

The developed multi-harmonic state-space modelling procedure, possible due to the estimations of the MHDTF, provided a clear improvement by considering the higher-orders contributions, however, its accuracy is only at the level of excitation used during the identification, due to the underlying linearisation. To this prediction, the use of Polymax and MLMM to obtain a good fit of the higher-order NLFRC should be further investigated. However, the underlying linearisation does not allow to obtain a good model behaviour at arbitrary excitation amplitudes. To overcome this limitation, the model in equation Equation 3(a) and Equation 3(b) should include additional terms to account for the nonlinearity.

Acknowledgements

The author would like to thank Instituto Superior Técnico and Professor Nuno Silvestre for granting me the opportunity of taking this endeavour. I am also very grateful of Eng. Giancarlo Kosova, who closely guided me these last months. Without his expertise and dedication this work wouldn't be possible.

I also have to thank Siemens Digital Industries Software for the internship opportunity. I could not have asked for a better environment to develop from.

References

[1] W. Heylen, S. Lammens, P. Sas, Modal Analysis Theory and Testing, Katholieke Universteit Leuven, Departement Werktuigkunde, Leuven, 2005.

[2] G. Gloth, M. Sinapius, Analysis of swept-sine runs during modal identification, Mechanical Systems and Signal Processing 18 (6) (2004) 1421–1441, doi:10.1016/S0888-3270(03)00087-6.

[3] U. Musella, E. Faignet, B. Peeters, P. Guillaume, Digital tracking techniques for mimo swept sine control testing, in: Proceedings of International Conference on Noise and Vibration Engineering (ISMA), Leuven, Belgium, 2020.

[4] Zurich Instruments, Principles of lock-in detection and the state of the art, White Paper (Nov. 2016).

[5] G. Kerschen, K. Worden, A. F. Vakakis, J.-C. Golinval, Past, present and future of nonlinear system identification in structural dynamics, Mechanical Systems and Signal Processing 20 (3) (2006) 505–592, doi:10.1016/j.ymssp.2005.04.008.

[6] G. Kerschen, M. Peeters, J. Golinval, A. Vakakis, Nonlinear normal modes, Part I: A useful framework for the structural dynamicist, Mechanical Systems and Signal Processing 23 (1) (2009) 170–194, doi:10.1016/j.ymssp.2008.04.002.

[7] G. Abeloos, L. Renson, C. Collette, G. Kerschen, Stepped and swept control-based continuation using adaptive filtering, Nonlinear Dynamics 104 (2021). doi:https://doi.org/10.1007/s11071-021-06506-z.

[8] T. Detroux, L. Renson, L. Masset, G. Kerschen, The harmonic balance method for bifurcation analysis of large-scale nonlinear mechanical systems, Computer Methods in Applied Mechanics and Engineering 296 (2015) 18–38, doi:10.1016/j.cma.2015.07.017.

[9] R. All, Digital Filters For Everyone, 3^{rd} Edition, Creative Arts & Sciences House, 2015.

[10] J. Moorer, The Manifold Joys of Conformal Mapping: Applications to Digital Filtering in the Studio, Journal of the Audio Engineering Society 31 (11) (1983) 826–841.

[11] B. Peeters, H. V. der Auweraer, P. Guillaume, Jan-Leuridan, The polymax frequency-domain method: A new standard for modal parameter estimation?, Shock and Vibration 11 (2004) 395–409, doi:10.1155/2004/523692.

[12] M. El-kafafy, G. Accardo, B. Peeters, K. Janssens, T. De Troyer, P. Guillaume, A Fast Maximum Likelihood-Based Estimation of a Modal Model, in: M. Mains (Ed.), Topics in Modal Analysis, Volume 10, Springer International Publishing, Cham, 2015, pp. 133–156, doi:10.1007/978-3-319-15251-6_15.

[13] M. Elkafafy, B. Peeters, Robust Identification of Stable MIMO Modal State Space Models, in: B. J. Dilworth, T. Marinone, M. Mains (Eds.), Topics in Modal Analysis & Parameter Identification, Volume 8, Springer International Publishing, Cham, 2023, pp. 81–95, doi:10.1007/978-3-031-05445-7_10.